

Cortical aperiodic ‘clock’ enabling phase transitions at theta rates

Proceedings International Joint Conference on Neural Networks, Orlando FL, 12-17 August 2007. Abstract # 1323

Walter J Freeman, *Life Fellow, IEEE*

Abstract — Brains are open thermodynamic systems, continually dissipating metabolic energy as heat in constructing spatiotemporal patterns of neural activity. Here observations on patterns of cortical oscillations are described as Prigogine’s “dissipative structures” forming at conditionally stable operating points far from equilibrium. The approach is to locate experimentally a small-signal, near-linear range in which impulse responses superpose, then to extend the analysis into nonlinear ranges by piece-wise linearization. The resulting root loci are re-interpreted as projections from a phase plane, in which the phase boundaries are plotted in terms of degree of order corresponding to volume vs. rate of energy dissipation (power) corresponding to temperature. Properties of neural microscopic activity transit across scales to macroscopic states.

I. INTRODUCTION

The spontaneous background activity of the cerebral cortex is well known to contain a broad range of frequencies of oscillation. Commonly these ranges are described in terms of clinical bands, among which are theta-alpha (3-12 Hz) and beta-gamma (12-80 Hz). In subjects at rest the power spectral densities (PSD) commonly conform to “ $1/f^\alpha$ noise” with the exponent α ranging between 2 and 3. These signals are commonly analyzed by linear decomposition (e.g., FFT, PCA, ICA, ARMA, etc.) despite the lack of stationarity as evidenced by modulations of signals in both frequency and phase. Use of the Hilbert transform decomposes ECoG signals into analytic amplitude and phase. The square of analytic amplitude gives an index of cortical expenditure of free energy, because it is determined by the flow of dendrite current across fixed tissue resistance, giving mean power, $\underline{A}^2(t)$, equal to the square of current density times the specific resistance. Multiple simultaneous recordings from 64 electrodes give spatial patterns of ECoG activity, each of which can be represented as a point in 64-space. Sequential points represent trajectories in 64-space, $D_c(t)$, and clusters from ECoG of sensory cortices represent patterns that are correlated with perceptions of conditioned stimuli (CS). The pragmatic information, $H_c(t)$, in a cluster or trajectory of points can be estimated by the ratio of the analytic power to the rate of change in the Euclidean distance, $D_c(t)$, constituting an order parameter, $H_c(t) = \underline{A}^2(t) / D_c(t)$ [1-4].

Repetitive sampling of the environment by subjects in each sensory modality (olfaction, vision, hearing and touch) is expressed as action-perception cycles, by which animals and humans learn about the environment. Each sniff, saccade or whisker sweep may be accompanied by an abrupt change in cortical dynamics that can be modeled as a state transition. If the state of the cortex can be shown to conform to that of self-organized criticality, then the resulting

pseudo-equilibrium allows portrayal of the cortical dynamics of receiving, transmitting and seizure states of cortex as different phases, with phase transitions between them. The critical point is identified with a self-stabilizing pole at the origin of the complex plane manifesting a non-zero point attractor. The phase boundary between receiving and transmitting cortical states corresponds to the imaginary axis. The action-perception cycle manifested in the respiratory act of sniffing at theta rates is plotted as a torus (projection of a helix in time). This cycle is evaluated by measurements of the spatiotemporal patterns of the electrocorticogram (ECoG) in trained cats and rabbits. The data show that the critical event in perception is a phase transition by which a discontinuity occurs in cortical dynamics, when a singularity emerges by the intrinsic near-zero decrease in analytic power superimposed on a surge of excitatory input from sensory receptors. Thereby order emerges from disorder having the illusory appearance of chaos. The resulting phase portrait incorporates conditional stability relating to ‘metastability’ [5], the discontinuity in analytic phase at the onset of a state transition into the transmitting state, and the return to the receiving state without a discontinuity in the temporal dynamics.

II. LINEAR ANALYSIS OF CORTICAL DYNAMICS IN RESTING

Neurons in cortex must be continually active in order to survive. Their electrical activity is observed in two forms: waves of dendritic synaptic current that establish weak standing fields of potential as dendritic synaptic current flows across the fixed extracellular resistance of cortex, and trains of action potentials on axons that are treated as point processes. Pulse densities are monotonically dependent on wave current densities. The range is bounded by threshold at the low end and refractoriness at the high end, with a near-linear small-signal range. Demonstration of this operating range is by paired-shock perturbation to test for additivity and proportionality in superposition [6].

The dendrites of the typical neuron integrate the pulse trains from 10^4 input neurons and transmit to 10^4 other neurons. So high is the packing density of cortical neurons ($10^5/\text{mm}^3$) that a neuron connects with only 10^{-2} neurons within its dendritic radius. The chance of forming a dyadic pair is 10^{-6} . Hence each neuron interacts with its surround, predominantly by mutual excitation, because ~85% of its synapses are excitatory. The anatomical connection density is sufficiently high that each neuron can receive more pulses per unit time than it transmits, but its capacity to transmit is limited by its refractory periods. That limit provides for the robustness of steady-state background activity in both pulse and wave modes (Fig. 1), and for the continuing stability in the face of major increases in arousal, such as occur in highly motivated animals on the transition from waking rest to active search (Fig. 1, A).

Walter J Freeman is Professor Emeritus of Neurobiology in the Dep’t of Molecular & Cell Biology, University of California at Berkeley CA 94720 USA. Correspondence to dfreeman@berkeley.edu, tel 1-510-642-4220, fax 1-510-643-9290. Download cited papers from: <http://sulcus.berkeley.edu>

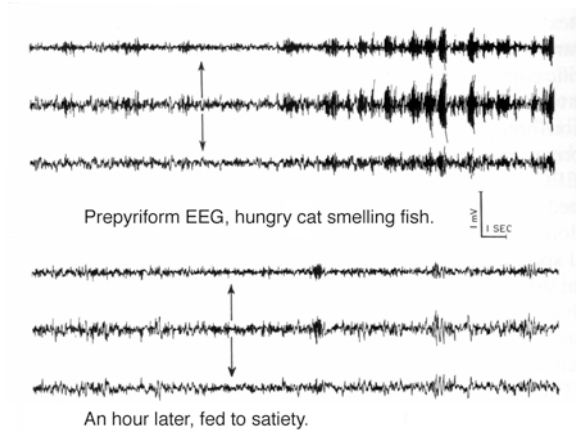


Fig. 1. A. A food-deprived cat at rest is aroused by an odor of fish. B. After satiety there is no arousal. Freeman (1975/2004) Fig 7.17 p 442.

Mutual excitation is described by ordinary differential equations (ODE), in which a population of neurons is divided into a receiving subset and a transmitting subset that is continually renewed. Each subset is described by a 3rd order ODE representing the synaptic and cable delays of membranes and the passive resistance-capacitance of the membrane [6]. The ODE are evaluated by measuring the impulse responses (Fig. 2, A) to electric shocks given to the afferent axons into an excitatory population (a KLe set).

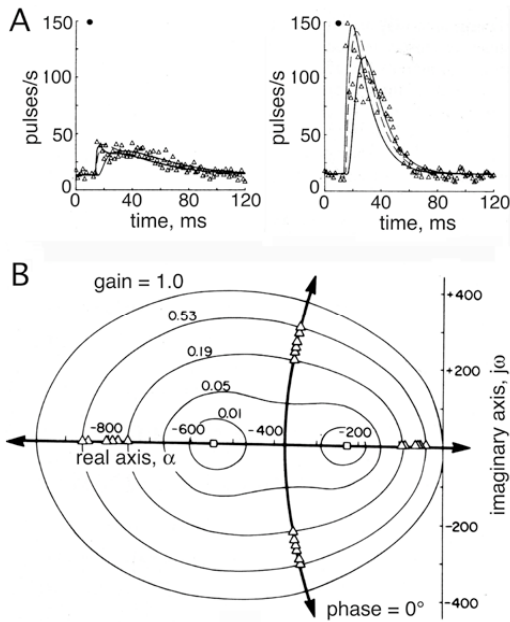


Fig. 2. A. Impulse responses of mutually excitatory neurons for low and high input intensity. B. The fitted curves in A are sums of exponentials in sets of coupled linear ordinary differential equations (ODE) that give the eigenvalues shown in the complex plane, from which a stable point attractor at the origin, 0,0, (not shown here) is inferred by linear extrapolation to zero amplitude of input and zero decay rate of the response. Freeman (1975/2004) Fig. 5.10 p 289, Fig 5.13 p 292.

These properties account for the stability of local areas of cortex and for the whole cerebral cortex without need for inhibition. The role of inhibition is to provide for the possibility of oscillation in the beta-gamma range (12-80

Hz), which is described by an 8th order ODE in a KII set formed by the interaction of a KLe set and a KIi set. An example of the impulse response to an afferent electrical stimulus that is recorded with an 8x8 (3.5x3.5 mm) array of electrodes (Fig. 3, A) shows an oscillation at a fixed frequency near 50 Hz with an exponential decay of the envelope that monotonically increases in proportion to response amplitude. The parameterized ODE give root loci that demonstrate increased stability with increasing amplitude (Mode 1e, Fig., 3, B).

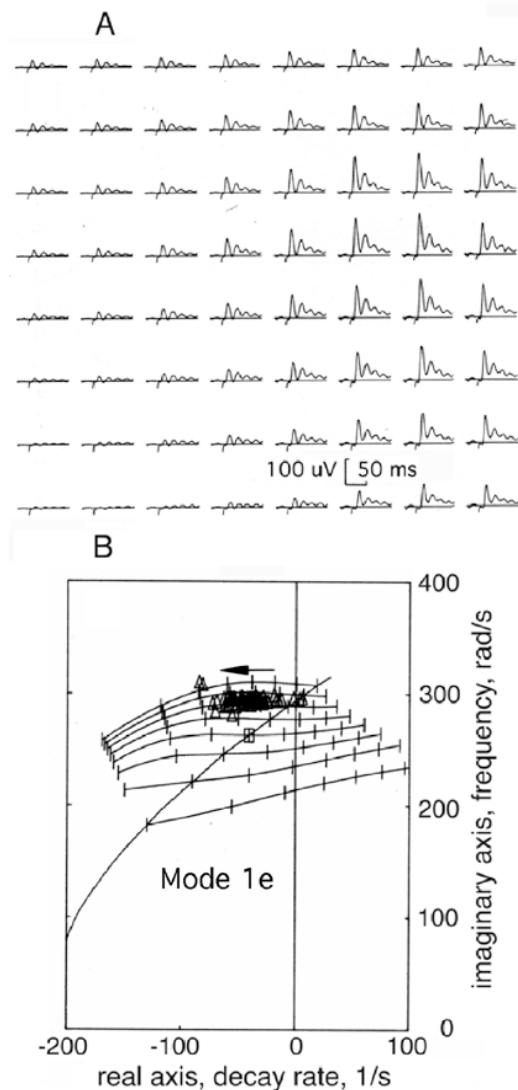


Fig. 3. A. A set of 64 simultaneously derived impulse responses from an ECoG array gave different amplitudes for single-shock stimuli of the nerve to the olfactory bulb, but oscillations all at the same frequency, with decay rates proportional to amplitude [as in Fig. 1, A]. B. The eigenvalues of the dominant damped cosine wave that was fitted to each of the 64 impulse responses gave root locus Mode 1e in KII set. Mode 1e shows the increased stability imposed by the bulbar mechanism in response to irrelevant and noisy input. Freeman (1975/2004) Fig. 4.27 p 221, Fig 6.86 p 361.

These properties were seen only when the response amplitude was driven to exceed the self-regulated amplitude of the spontaneous activity. When the magnitude of the impulse input was fixed to give an impulse response with

peak amplitude below the background range, then by averaging over many trials a different pattern of variation emerged, in which with increasing amplitude the decay rate decreased, implying mere conditional stability and the possibility of a state transition from a decaying envelope to an exponentially increasing envelope of oscillation, but with bounding by reflection back to the imaginary axis.

This configuration predicts the existence of a limit cycle attractor near 40 Hz (Mode 2, Fig. 4). It is the basis for describing cortex as a bistable system that switches rapidly from a receiving mode to a transmitting mode and back again, much as an axon switches between its resting state and its transmitting state in generating an action potential.

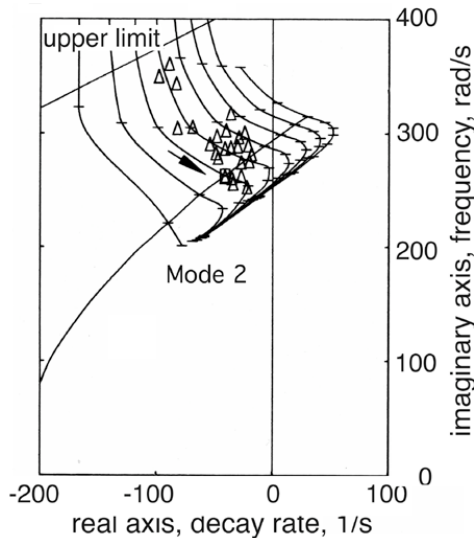


Fig. 4. When input intensity is fixed at a low level, so that peak amplitude of the impulse response is less than the range of the background activity, the amplitude of the impulse response fluctuates spontaneously, and likewise the frequency and decay rate, but in the direction of decreased stability, reflecting the tendency of the system to cross the imaginary axis and enter into a predicted sustained oscillation near 40 Hz implying a limit cycle attractor in the gamma range. Freeman (1975/2004) Fig 6.21 p 374.

The increase in amplitude that is correlated with increased duration of the oscillatory impulse response (Mode 2, Fig. 4) implies a requisite increase in the rate of dissipation of metabolic energy by cortical neurons. This can be directly indexed by the mean square EEG amplitude, which is dependent on the dendritic current density flowing across the extracellular resistance. The increase in energy release is due to the fundamental property of a neuron, that the closer it is brought to threshold the more likely it is to fire. Most cortical neurons spend 99.9% of their lifetimes with their membrane potentials just below threshold. Fluctuations resembling thermal noise from mutual excitation bring them to fire at intervals with Poisson distributions having the brief dead time owing to refractoriness. This nonlinear property is expressed in the asymmetry of the sigmoid curve [7]: the maximal slope is displaced to the excitatory side of wave input, so that excitation increases both output amplitude and the positive feedback gain, which enhances the conditional instability by approaching the boundary represented by the imaginary axis.

In contrast, the impulse stimulation of the outflow path of the bulb bypasses the excitatory KIE population at its input and fails to deliver the excitatory bias that is seen in the baseline shift of orthodromic impulse responses (Fig. 3, A). Instead, an inhibitory bias is revealed that results in a root locus rotated 90° counter-clockwise (Fig. 5), in which the decay rate is relatively constant with increased amplitude, while the frequency very strongly decreases. This pattern is designated Mode 1i; it is due to block of transmission in the negative feedback loop, which reduces the feedback gain.

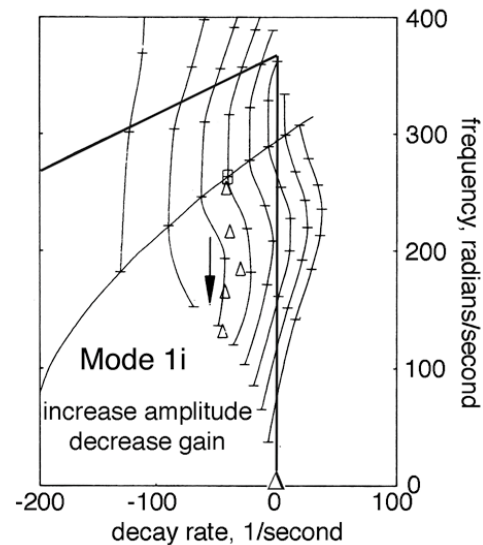


Fig. 5. The root locus is shown for antidromic stimulation of the olfactory bulb in the absence of excitatory bias. Freeman (1975/2004) Fig 6.11 p 374.

Every time an animal sniffs or moves its eyes or other parts of its body, it triggers a burst of sensory input that increases the gain. However, that increase may not suffice to push the cortex across the boundary. Other factors are required. One is the increase in the positive feedback gain, K_p , in the KIE set at the entry to sensory cortex, which rises with augmented arousal (Fig. 2). Another factor is a selective increase in synaptic strength between co-active neurons during reinforcement learning in accord with the Hebb Rule: neurons that fire together 'wire' together. A motivated animal that receives a recognizable sensory stimulus is primed, so that a very small increase in sensory excitation can provide the necessary energy for the system to cross from the small-signal, near-linear domain of the receiving state into the high-energy transmitting state.

When that happens in the olfactory, visual, auditory or somatosensory cortex, two spatiotemporal patterns emerge: a spatial pattern of amplitude modulation (AM) and a spatial pattern of phase modulation (PM) of the shared carrier frequency of the oscillation in the transmitting state [3, 4]. The AM patterns are most readily observed in contour plots of the root mean square amplitudes of 64 signals, which reflect the differences occasioned by learning to recognize different stimuli. Quantitative assay is by expressing each

frame with a 64x1 feature vector that specifies a point in 64-space from 64 root mean square amplitudes. Visualization requires statistical analysis such as stepwise discriminant analysis or nonlinear mapping for display in 2-D, in which similar patterns form clusters [3]. Each cluster manifests a chaotic attractor that corresponds to a category of CS that an animal has learned to recognize, and which is surrounded by a basin of attraction that corresponds to the generalization gradient for that category. These basins and their attractors are latent prior to the onset of a state transition. The attractor landscape is actualized by an act of observation (sniff, glance, etc.), upon which the incoming CS selects one and only one basin, in which the convergence to the attractor executes the fundamental perceptual processes of abstraction and generalization.

The state transitions and their attendant AM and PM patterns tend to recur at rates of 3-10 Hz (the theta-alpha range) in each sensory area. Classifiable AM patterns typically last 60-120 ms (3-5 cycles of the carrier frequencies of 12-30 Hz, the beta-gamma range). Examination of the state transitions in greater detail requires finer temporal resolution. This is provided by the Hilbert Transform, which decomposes the EEG into two independent signals: the instantaneous analytic power, $A_j^2(t)$, for the j -th channel and the instantaneous analytic frequency, $\omega_j(t)$. Two parameters derived from these signals are compared in Fig. 6. The spikes show the spatial standard deviation, $SD_j(t)$, of $\omega_j(t)$. The increase in $SD_x(t)$ reflects the abrupt temporal discontinuity as the cortex switches from one phase pattern (PM) to the next but at slightly different times, so it provides a useful marker for the times of onset and recurrence rates of sensory-dependent state transitions. The ratio of the square of the analytic amplitude to the rate of change in spatial pattern gives the pragmatic information $H_c(t)$. This quantity serves as an order parameter for cortical dynamics [1-4] in forming AM patterns, which are instantiations of Prigogine's "dissipative structures" [8].

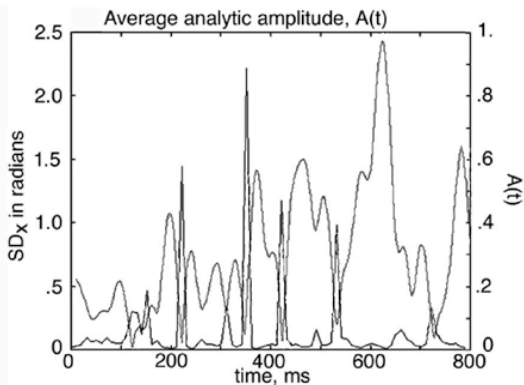


Fig. 6. The black spikes reflect the times at which the phase becomes indeterminate, reflecting a discontinuity in the analytic phase when the analytic amplitude (gray curve) goes to a minimum. After the spike in the spatial SD of phase differences falls, the rate of change in the spatial pattern of amplitude, $D_c(t)$, goes to a minimum (Fig. 7 grey curve) before the analytic amplitude increases. The important point is that order increases after an approach of the analytic amplitude toward zero. Freeman (2004a) Fig 1.01, A..

The gray curve shows the mean power, $\underline{A}^2(t)$, or rate of energy dissipation, which tends to a minimum during the maxima for $SD_j(t)$ and to a peak during the plateau that reflects relative constancy in $\omega(t)$ and therefore stationarity in cortical dynamics during the frame with peak power. The feature vector, $\mathbf{A}^2(t)$, given by the square of the normalized analytic amplitude specifies the spatial pattern and therefore serves as the order parameter for describing the system, the control parameter being the level of sensory input. The Euclidean distance between successive points in 64-space specified by $D_c(t) = |\mathbf{A}^2(t) - \mathbf{A}^2(t-1)|$ serves as an index of the rate of change in spatial pattern (grey curve, Fig. 7). Its reciprocal, $1/D_c(t)$, times $\underline{A}^2(t)$ gives $H_c(t)$, a scalar index of the order parameter: very short steps between successive values of $\mathbf{A}^2(t)$ indicate prolonged AM pattern stability.

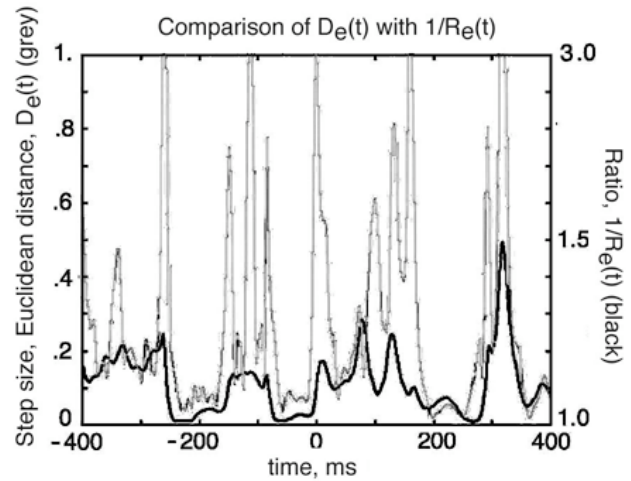


Fig. 7. Phase synchronization, $R_c(t)$, precedes pattern stabilization, $D_c(t)$. Both precede mean power increase, $\underline{A}^2(t)$. Freeman (2004a) Fig. 103, A.

IV. DESCRIPTION OF CORTEX AS A THERMODYNAMIC SYSTEM SELF-STABILIZED FAR FROM EQUILIBRIUM

The mean square amplitude, $\underline{A}^2(t)$, does not by itself suffice to specify power (current density squared times specific tissue resistance). Fluctuations in resistance were ruled out by passing a fixed current at 1 KHz across the tissue and showing no significant variation in transcortical potential at that frequency. Fluctuations in the degree of synchrony were shown not to cause the rise in $\underline{A}^2(t)$ to a peak by temporal standard deviations, $SD_T(t)$, across a time window twice the duration of the center wavelength of the pass band required for computation of the Hilbert Transform. The ratio, $R_c(t)$, was calculated of the $SD_{T,x}(t)$ of the spatial average filtered waveform divided by the spatial average $\underline{SD}_T(t)$, which ranged from 1 for perfect synchrony to $1/n^{0.5}$, where n was the number of data points in the window. $R_c(t)$, (the black curve in Fig. 7 showing the reciprocal) was found to increase before the increase in $\underline{A}^2(t)$ began and to hold steady as mean power continued to increase and then decrease. $R_c(t)$ served as a measure of cortical efficiency, on the premise that cancellation of oscillations in a population with phase dispersion would not process information [4].

Two state variables are adopted here to describe the thermodynamics of cortex operating as an open system far from equilibrium: $\underline{A}^2(t)$ representing mean power in analogy to temperature in a thermodynamic system at equilibrium, and $H_c(t) = \underline{A}^2(t) / D_c(t)$, indexing the order parameter in analogy to volume or pressure (Fig. 8, A). Three features are most important. There are three phases separated by two phase boundaries. An increase in power (temperature) is accompanied by a decrease in order. In addition to the triple point there is a “critical point” at which one of the phase boundaries disappears.

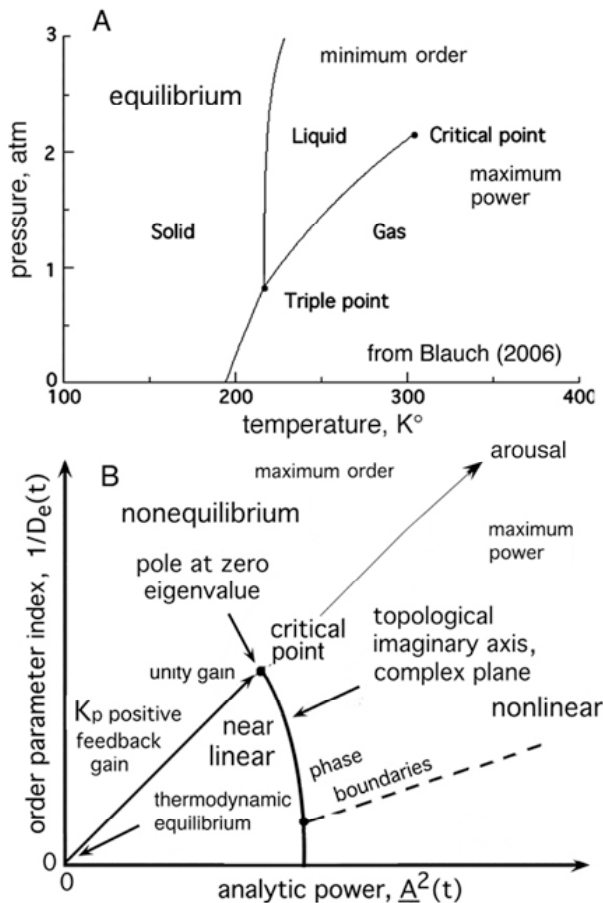


Fig. 8. A. The classic phase portrait of a substance at equilibrium [9] shows the three phases at equilibrium, separated by phase boundaries. The degree of order decreases with increasing power. Beyond the critical point the particles cannot be defined as belonging to either phase. **B.** In adapting these conventions to states far from equilibrium, the critical point is related to the pole at the origin of the complex plane, and the phase boundary is related with the imaginary axis. However great the degree of arousal and the level of the pulse density output of the excitatory populations, the neurons are always kept in the steady state at unity gain by refractory periods. Therefore, the critical point is identified with self-organized criticality [10], which can help explain the conditional stability of the cortical dynamics.

In a nonequilibrium description of cortex the equilibrium state is reduced to a point at the origin (Fig. 8,B) where the EEG is flat and $K_p = \underline{A}^2(t) = 1/D_c(t) = 0$. This “open loop” state occurs reversibly under deep anesthesia and irreversibly in death. In normal brain function K_p is always self-stabilized at unity gain, yet with a variable level of background activity that depends on neurohumoral control

of a corresponding expenditure of energy (Fig. 1, A) and an increase in order owing to distributed interactions that constrain (“enslave” in Haken’s term [11]) the activity of the constituent neurons (the diagonal arrow, Fig. 8, B). The thermodynamic critical point is identified with the zero eigenvalue shown by the pole that is inferred to exist at origin of the complex plane (Fig. 2, B). The adjoining phase boundary corresponds topologically to the imaginary axis, which separates the near-linear receiving state to the right from the nonlinear, transmitting state to the left. Also to be considered elsewhere is the inferred existence of another phase boundary separating these normal states from the state of epileptic seizure [12].

The critical point is not observed directly but is inferred by extrapolation of the decay rates of impulse responses to zero decay rate at zero amplitude in Mode 1. Omnipresent input from sensory receptors throughout the body displaces the rest point to a higher energy level and a lower degree of order (Fig. 9, A, upper left triangle to lower right triangle). From this rest point extend the root loci for Modes 1e, 1i, and 2. Owing to widespread excitatory and inhibitory interactions among cortical areas the observed activity appears “chaotic”. Actually the activity is constrained, band pass filtered noise from mutual excitation that forms a non-convergent attractor masquerading as chaos. Power spectral densities at rest commonly tend toward brown noise ($1/f^2$) black noise ($1/f^3$) [4], which is readily simulated by summing over many time series of independent random numbers. This can account for the variation that is observed in the impulse responses giving Mode 2. The requirement for reducing the background rate of energy dissipation to induce a phase transition is immediately apparent, so that the foreground burst of energy provided by receptors, a small fraction of the total release of cortical energy, can be enabled play its crucial role in selecting the basin of attraction that is appropriate for the incoming sensory information [3-4].

V. CONCLUSIONS

A fully competent and comprehensive approach to brain dynamics will require coordination of diverse theoretical and experimental approaches that include the several hierarchical levels at which brains function and can be observed and also manipulated. Bridging the levels, as between microelectrode recordings of units and LFP, and between ECoG or EEG and fMRI, is among the greatest challenges faced today by neuroscientists, one that has already been surmounted by physicists in their domain. This review maps terms and concepts between classical nonequilibrium thermodynamics [8], synergetics [9], many-body physics [13], random graph theory [14], neuropercolation [14], and neurodynamics [7]. These diverse disciplines give neurobiologists new tools and physicists new approaches to brain dynamics in the attempts to understand the neurodynamics of perception.

Of greatest importance in the display of the perceptual phase transition in Fig. 9 is the decrease in power that

precedes the formation of a new AM pattern (in the direction of the arrow for Mode 2, which reflects the the reduction in amplitude of the ‘spontaneous’ background activity in contrast to increased sensitivity caused by input). Selection by a weak CS of a basin of attraction requires that the noise level in the cortex drop dramatically in the presence of the input volley. That decrease repeats independently like a shutter in the theta-alpha range as an intrinsic property of the microscopic discharges [4] in the genesis of the “noise” by KIE sets and its band pass filtering by KII sets (Fig. 10). This insight, which is provided by this thermodynamic description of root loci in cortical dynamics, offers a key to understanding the control of macroscopic behavior by the microscopic dynamics of interacting neurons.

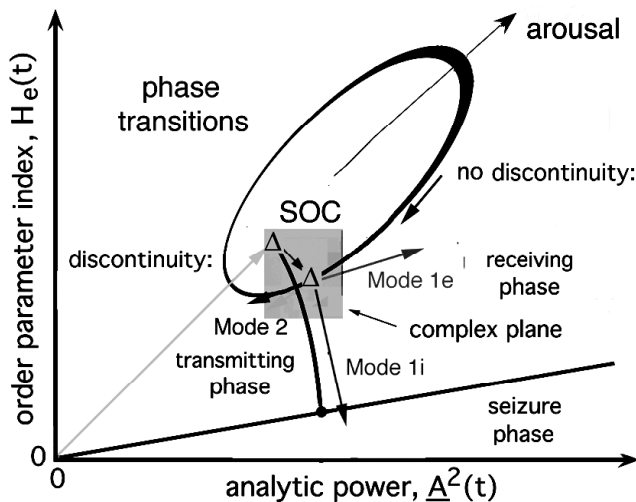


Fig. 9. The action-perception cycle is shown in the coordinates of degree of order as a function of rate of dissipation of free energy. This cycle repeats with each sniff or saccade. The growth of the dissipative structures [8] detected and measured as AM patterns occurs first by a decrease in power and order occasioned by the aperiodic emergence of a singularity in the background noise [4] that sets the stage for a phase transition. The surge of input from sensory receptors that contains information in the form of a CS can then select which attractor in the learned attractor landscape is relevant to the moment and the intent of the subject by which the sampling of the environment is guided. The gray area at the center shows the area of the complex plane from linear analysis, and the three arrows reflect the experimental root loci derived by parametric variation of the strength of the impulse used to get the impulse responses.

The hypothesis is proposed that brown noise from mutual excitation in KIE sets, when filtered at the characteristic frequencies of KII sets in the beta and gamma ranges, generates repeatedly an intrinsic temporary global reduction in analytic power, which constitutes a type of singularity in the temporal dynamics, at which the phase is undefined. This ‘pause’ in the cortical system introduces an opportunity for a phase transition, which is then triggered or governed by the prevailing sensory or extracortical input at the moment of the singularity, owing to the sensitization to afferent input that is described by Mode 2. Thus the background ‘noise’ intrinsically provides for an aperiodic ‘clock’ or ‘shutter’ for the repetitive formation of new opportunities for phase transitions at rates in the theta and possibly alpha ranges. Content in output of AM patterns is then the expression of accumulated synaptic modifications from prior learning.

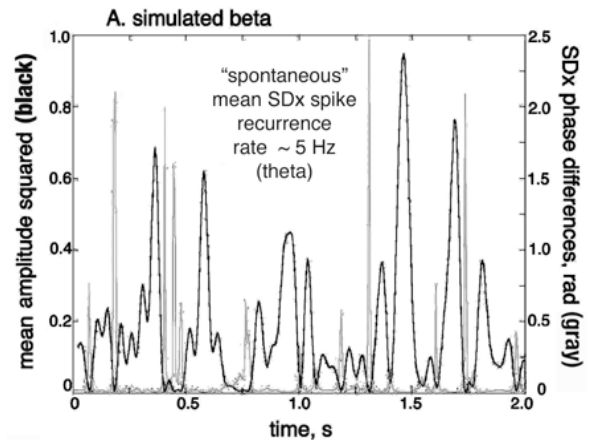


Fig. 10. The inverse relation between mean analytic power (amplitude squared, $\underline{A}^2(t)$) and the spatial standard deviation of the instantaneous phase differences (analytic frequency), $SD_x(t)$ is simulated with the sum of i.i.d. random numbers representing brown noise ($1/t^2$). The average repetition rate of the minima in $\underline{A}^2(t)$ where analytic phase is undefined is in the theta range as in the observed ECoG [4]. From Freeman (2006) Fig. 3, A, p 578.

REFERENCES

- [1] W. J. Freeman. “Origin, structure, and role of background EEG activity. Part 1. Analytic amplitude”. *Clin. Neurophysiol.* 115: 2077-2088, 2004.
- [2] W. J. Freeman. “Origin, structure, and role of background EEG activity. Part 2. Analytic phase”. *Clin. Neurophysiol.* 115: 2089-2107, 2004.
- [3] W. J. Freeman. “Origin, structure, and role of background EEG activity. Part 3. Neural frame classification”. *Clin. Neurophysiol.* 116 (5): 1118-1129, 2005.
- [4] W. J. Freeman. “Origin, structure, and role of background EEG activity. Part 4. Neural frame simulation”. *Clin. Neurophysiol.* 117/3: 572-589, 2006.
- [5] S. L. Bressler and J. A. S. Kelso. “Cortical coordination dynamics and cognition. *Trends Cognitive Sci.* 5: 26-36, 2001.
- [6] W. J. Freeman (1975) *Mass Action in the Nervous System*. Academic Press, New York, 1975. Reprinted 2004: <http://sulcus.berkeley.edu/MANSWWW/MANSWWW.html>.
- [7] W. J. Freeman. *Neurodynamics. An Exploration of Mesoscopic Brain Dynamics*. London: Springer-Verlag, 2000. <http://sulcus.berkeley.edu/2006>
- [8] I. Prigogine. *From Being to Becoming: Time and Complexity in the Physical Sciences*. San Francisco: W. H. Freeman, 1980.
- [9] D. N. Blauch, http://www.chm.davidson.edu/Chemistry_Applets/, 2006
- [10] H. J. Jensen. *Self-Organized Criticality: Emergent Complex Behavior in Physical and Biological Systems*. New York: Cambridge University Press, 1998.
- [11] H. Haken. “What can synergetics contribute to the understanding of brain functioning?”, in: *Analysis of Neurophysiological Brain Functioning*. C. Uhl (Ed.) Berlin: Springer-Verlag, pp. 7-40, 1999.
- [12] W. J. Freeman, M. D. Holmes, G. A. West, S. Vanhatalo. Fine spatiotemporal structure of phase in human intracranial EEG. *Clin. Neurophysiol.* 117, 6, 2006, pp 1228-1243, 2006.
- [13] W. J. Freeman and G. Vitiello. Nonlinear brain dynamics as macroscopic manifestation of underlying many-body dynamics. *Physics of Life Reviews* 3: 93-118, <http://dx.doi.org/10.1016/j.plrev.2006.02.001>, <http://repositories.cdlib.org/postprints/1515>, 2006
- [14] B. Bollobás. “Random graphs”. *Cambridge Studies in Advanced Mathematics 2nd Edition*. Cambridge UK: Cambridge University Press, xviii+498 pp, 2001.
- [15] R. Kozma, M. Puljic, P. Balister, B. Bollobás and W. J. Freeman. Phase transitions in the neuropercolation model of neural populations with mixed local and non-local interactions, *Biological Cybernetics*, Vol. 92, pp. 367-379, 2005.